

A. Forgiarini  
J. Esquena  
C. González  
C. Solans

## Formation and stability of nano-emulsions in mixed nonionic surfactant systems

---

A. Forgiarini · J. Esquena · C. Solans (✉)  
Dept. Tecnologia de Tensioactius  
Institut d'Investigacions Químiques  
i Ambientals de Barcelona, CSIC, Jordi  
Girona 18-26, 08034 Barcelona, Spain  
e-mail: csmqci@cid.csic.es  
Tel.: + 34-93-4006159  
Fax: + 34-93-2045904

C. González  
Dept. Enginyeria Química i Metal·lúrgica  
Universitat de Barcelona, Martí  
i Franquès 1, 08028 Barcelona, Spain

A. Forgiarini  
Facultad de Ingeniería, Universidad  
de Los Andes, Mérida 5101, Venezuela

**Abstract** The formation of nano-emulsions has been studied in water/mixed nonionic surfactant/oil systems using two emulsification methods. In one method, the composition was kept constant and the temperature was changed (phase-inversion temperature, PIT, method), while in the other method, water was added dropwise to a solution of the mixed surfactants in oil at constant temperature (method B). The droplet size and stability were determined as a function of surfactant mixing ratio,  $W_1$ , at 25 °C. The droplet size of nano-emulsions obtained by the PIT method is practically independent of  $W_1$  and falls in the range 60–80 nm. In contrast, the droplet size of nano-emulsions prepared by method B, is highly dependent on  $W_1$  and varies between 60 and

300 nm. At  $W_1$  values where the PIT or the hydrophile–lipophile balance temperature ( $T_{HLB}$ ) of the system is close to 25 °C, the droplet sizes of the nano-emulsions are similar for both emulsification methods. There are three equilibrium phases of the latter compositions: an aqueous micellar solution or oil-in-water microemulsion ( $W_m$ ), a lamellar liquid-crystalline phase and an oil phase (O) in addition, these nano-emulsions showed higher kinetic stability than those with lower  $W_1$  values (higher  $T_{HLB}$ ) and consisting of two liquid phases ( $W_m + O$ ).

**Key words** Nano-emulsions · Emulsification · Phase-inversion temperature · Hydrophile–lipophile balance temperature · Mixed non-ionic surfactant

---

### Introduction

Emulsions are thermodynamically unstable liquid/liquid dispersions formed, generally, by water, oil and surfactant mixtures [1, 2]. The type of emulsion that forms in a water/poly(oxyethylene glycol) alkyl ether surfactant/oil system is highly dependent on temperature. At low temperatures, the surfactant is mainly soluble in water giving rise to emulsions of the oil-in-water (O/W) type. These emulsions separate into two liquid phases: an aqueous micellar solution or oil-in-water microemulsion ( $W_m$ ) and an excess oil phase (O) (Winsor I system). At high temperatures, the surfactant is preferentially soluble in oil and the emulsions are of

the water-in-oil (W/O) type. Two phases are also present at equilibrium: an aqueous phase (W) and a reverse micellar solution or W/O microemulsion phase ( $O_m$ ) (Winsor II system). At an intermediate temperature, the so-called hydrophile–lipophile balance (HLB) temperature ( $T_{HLB}$ ) or the phase-inversion temperature (PIT), the hydrophilic–lipophilic properties of the nonionic surfactant are balanced [3]. At the HLB temperature, a transition from O/W to W/O emulsions takes place. The emulsions consist of three liquid phases in single-surfactant systems at this temperature: excess water and oil phases and a bicontinuous microemulsion phase (D) (Winsor III system) [4–6]. It is well known that emulsions showing Winsor III phase

equilibria. (e.g. near or at the  $T_{HLB}$ ) are very unstable owing to the extremely low values of the interfacial tension between the different phases [7–11]. In a mixed nonionic surfactant system, the hydrophilic–lipophilic properties are dependent on the surfactant mixing ratio at constant temperature. In the dilute region of these systems, the structure of the third phase may be a bicontinuous microemulsion [4, 6] or a liquid-crystalline phase [12, 13].

Nano-emulsions are a class of emulsions with a droplet size in the range 50–500 nm and have attracted a great deal of attention in recent years because of their wide range of practical applications [14–16]. Nano-emulsions are, generally, stable against sedimentation or creaming, owing to their small droplet size. The main ageing process in nano-emulsion destabilization is usually Ostwald ripening [17, 18]. In Ostwald ripening the larger droplets grow at the expense of smaller droplets owing to the different Laplace pressure in droplets of different sizes. The Ostwald ripening rate, according to the Lifshitz, Slezov and Wagner theory [19–21] is given by  $\omega = dr^3/dt = 8C_\infty\gamma V_m D/9\rho RT$ , where  $r$  is the average droplet radius,  $t$  is time,  $\gamma$  is the interfacial tension,  $D$  and  $C_\infty$  are the diffusion coefficient and the solubility of the droplet phase material in the bulk phase, respectively,  $V_m$  its molar volume,  $\rho$  is the density and  $T$  the temperature. This equation predicts a linear relationship between  $r^3$  and  $t$ .

We have reported, recently, nano-emulsion formation in a water/technical grade nonionic surfactant/oil system, at certain W/O ratios, when water is added stepwise to an oil/surfactant mixture [22]. However, when oil is added to water/surfactant mixtures, nano-emulsions are not obtained. These results could not be explained in terms of the equilibrium properties since the final composition of the emulsions was the same. It was suggested that the phase transitions during emulsification could play a key role in nano-emulsion formation. In order to gain a better understanding of nano-emulsion formation, it was considered of interest to determine the relationship between the emulsification method, the nano-emulsion droplet size and stability in systems with mixtures of pure nonionic surfactant.

## Experimental

### Materials

Homogeneous nonionics surfactants, tetraethylene glycol dodecyl ether ( $C_{12}E_4$ ), tetraethylene glycol tetradecyl ether ( $C_{14}E_4$ ), tetraethylene glycol hexadecyl ether ( $C_{16}E_4$ ) and hexaethylene glycol dodecyl ether ( $C_{12}E_6$ ) were supplied by Nikko Chemicals Co (Japan). *n*-Decane (purity above 99%) and NaCl (purity above 99.5%) were obtained from Merck. Water was deionized by Milli-Q filtration.

### Methods

#### HLB temperature

$T_{HLB}$  was determined by conductivity with a Crison model 525 conductimeter, with a Pt/platinized electrode. The samples were prepared with an electrolyte solution (NaCl  $10^{-2}$  M) instead of pure water. The conductivity of samples with different surfactant mixing ratios was measured as a function of temperature.

#### Phase behavior

Samples with different surfactant mixing ratios and constant total surfactant concentration of 5 wt% and a W/O ratio of 80:20 were prepared and sealed in vials. The samples were stirred and kept in a thermostatted bath at 25 °C until equilibrium was reached. The presence of liquid-crystalline phases was detected by using crossed polarizers.

#### Emulsion formation

The emulsions were prepared by two low-energy emulsification methods (Fig. 1). In the PIT method the sample is kept at  $T_{HLB}$  and the O/W emulsion is obtained by quickly lowering the temperature to 25 °C. In method B, water is added little by little with agitation to a solution of surfactant plus oil at a constant temperature of 25 °C.

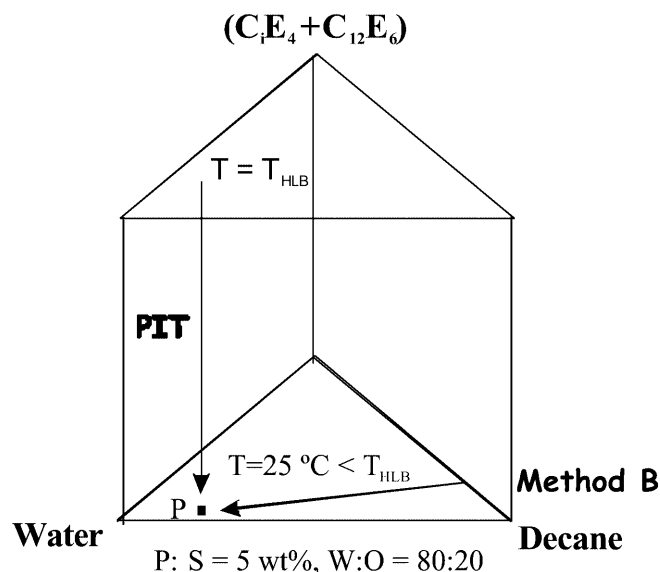


**Fig. 1** Schematic representation of two emulsification methods: phase-inversion temperature (PIT) and method B

#### Droplet size

The emulsion droplet size was determined by dynamic laser light scattering (Malvern 4700).

#### Stability

The emulsion stability was assessed by measuring the emulsion droplet size as a function of time at 25 °C.

## Results and discussion

### $T_{HLB}$ and emulsion type

Conductivity plots as a function of temperature are shown in Fig. 2 for one of the systems studied, water/( $C_{16}E_4 + C_{12}E_6$ )/decane, at three values of the surfactant mixing ratio,  $W_1$  (defined as the weight fraction of the most lipophilic surfactant over the total surfactant).

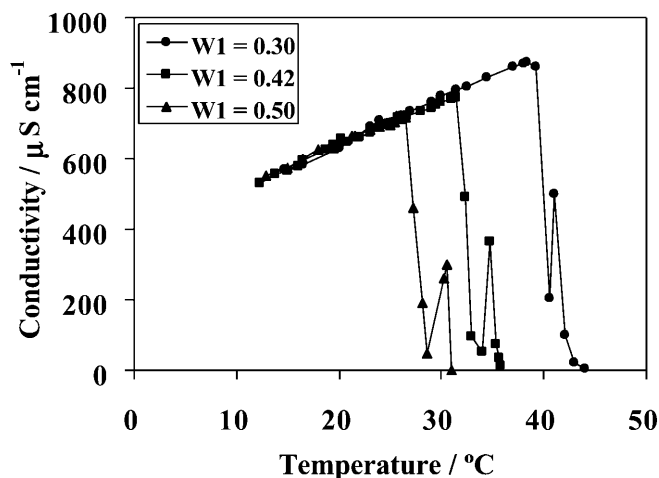


Fig. 2 Conductivity as a function of temperature for the system (aqueous solution  $10^{-2}$  M NaCl)/ $C_{16}E_4 + C_{12}E_6$ /decane. W/O = 80:20,  $S = 5$  wt%

Independently of the system, the features of the conductivity curves are similar: as the temperature increases, the conductivity initially increases slightly and then experiences an abrupt decrease to low values which is followed by an increase to intermediate values and a final decrease to very low values. The higher the  $W_1$  value the lower the temperature at which these drastic conductivity changes occur. Similar conductivity changes were described for the water/ $C_{12}E_4$ /decane system [23] and were related to the phase behavior of the system. Accordingly, the first drop in conductivity can be attributed to the formation of a lamellar liquid-crystalline phase and the following slight increase in conductivity to the formation of a bicontinuous microemulsion phase or an  $L_3$  phase. The overall conductivity changes indicate that emulsions invert from O/W to W/O via lamellar and bicontinuous phases. That is, the surfactant molecules change their affinity from water to oil or, in other words, the natural curvature of the surfactant changes from positive to negative through zero values of curvature [6, 24, 25]. In this work,  $T_{HLB}$  is taken as the mean temperature between the maximum and minimum values of conductivity. A linear relationship between  $T_{HLB}$  and  $W_1$  for the three water/( $C_iE_4 + C_{12}E_6$ )/decane systems studied,  $i = 12, 14, 16$ , is shown in Fig. 3. As expected,  $T_{HLB}$

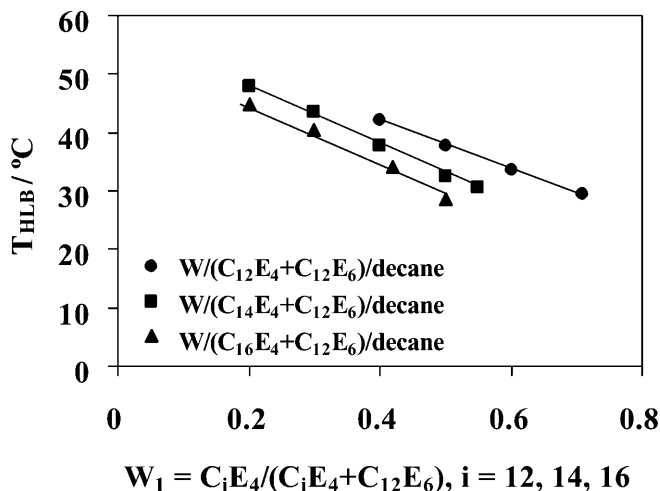


Fig. 3 Hydrophile-lipophile balance (HLB) temperature,  $T_{HLB}$ , as a function of surfactant mixing ratio,  $W_1$

decreases with the increase in the lipophilicity of the surfactant mixture [6, 12]. Since in water/nonionic surfactant/oil systems the emulsions are O/W below  $T_{HLB}$  and W/O above it, the emulsions reported in this work are of the O/W type at 25 °C and at the surfactant mixing ratios considered.

### Emulsification and emulsion droplet size

The emulsions were prepared according to the low-energy emulsification methods (PIT and method B) described in the Experimental section and shown schematically in Fig. 1. The droplet size of the emulsions obtained by the PIT method as a function of  $W_1$  is shown in Fig. 4. Independently of the system and the surfactant

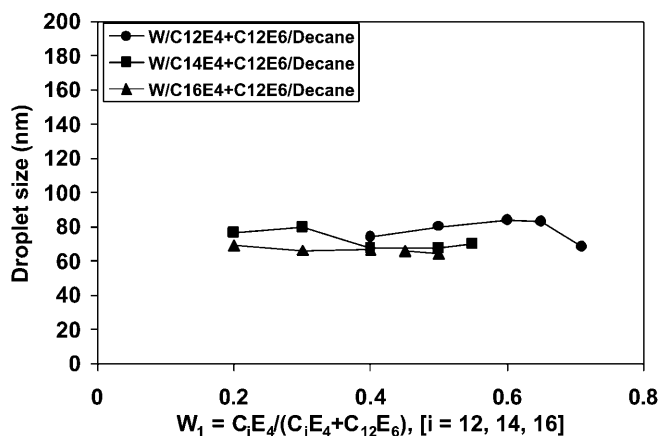


Fig. 4 Droplet size as a function of  $W_1$  obtained by the PIT emulsification method in water/( $C_iE_4 + C_{12}E_6$ )/decane systems

mixing ratio, the nano-emulsions obtained by this method have similar droplet size (between 60 and 80 nm). In contrast, the droplet size of emulsions obtained by method B depends on both the system and the surfactant mixing ratio (Fig. 5). Nevertheless, the

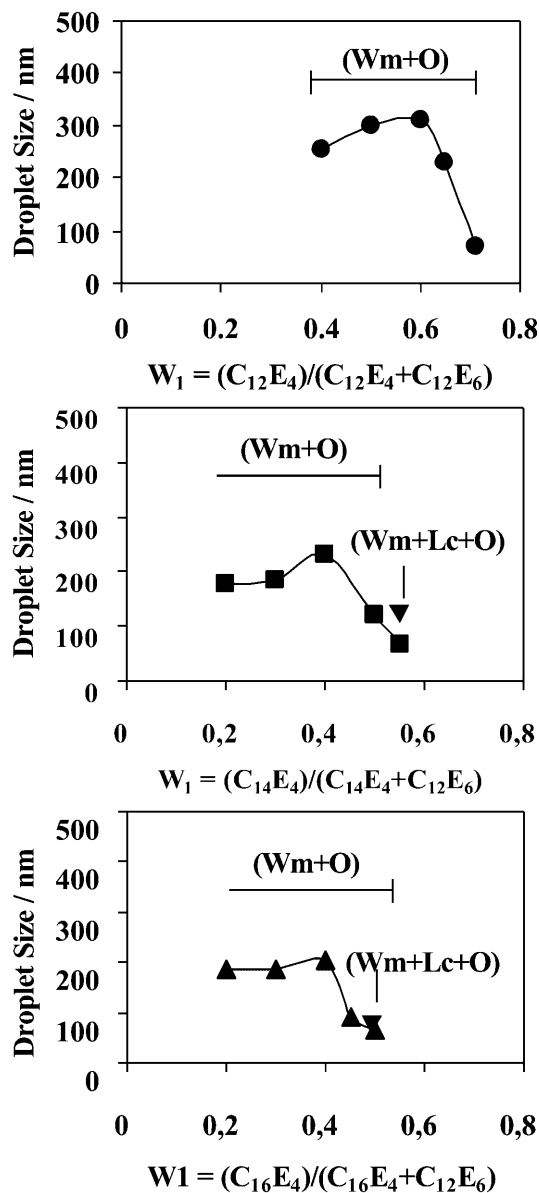


Fig. 5 Droplet size as a function of  $W_1$  obtained by emulsification method B in water/( $C_iE_4 + C_{12}E_6$ )/decane systems

tendency of the changes in droplet size versus  $W_1$  is similar: at low  $W_1$  (high hydrophilic surfactant content in the mixture), the droplet sizes are of the order of 150 nm; as  $W_1$  increases, the droplet sizes also increase reaching a

maximum, after which they decrease to values around 50 nm, of the same order as those obtained by the PIT method. The equilibrium phases present in the system are also indicated in Fig. 5. Emulsions belonging to the system with the most lipophilic surfactant,  $C_{12}E_4$ , consist of an O/W microemulsion phase ( $W_m$ ) in equilibrium with an excess oil phase (O) at all  $W_1$  studied. However, in the other two systems, water/( $C_{14}E_4 + C_{12}E_6$ )/decane and water/( $C_{16}E_4 + C_{12}E_6$ )/decane the phase equilibrium at  $W_1$  values where the smallest droplet sizes are obtained, consist of a lamellar liquid-crystalline phase ( $L_\alpha$ ) in equilibrium with  $W_m$  and O phases. It could be thought that the presence of the  $L_\alpha$  phase was the cause for the smallest values of the droplet size in nano-emulsions obtained by method B. However, in the system with  $C_{12}E_4$ , although the droplet sizes are as small as in the other systems, the  $L_\alpha$  phase is not present. The explanation of these results could lie in the fact that the  $T_{HLB}$  values of the compositions giving the smallest droplet sizes are very close to 25 °C, the temperature at which the emulsions are prepared.

Although the nano-emulsions obtained at compositions near  $T_{HLB}$  ( $W_1 = 0.70$  in  $C_{12}E_4 + C_{12}E_6$ ,  $W_1 = 0.55$  in  $(C_{14}E_4 + C_{12}E_6)$  and  $W_1 = 0.50$  in  $(C_{16}E_4 + C_{12}E_6)$  mixtures) showed similar droplet size, the stability of those belonging to the  $(C_{12}E_4 + C_{12}E_6)$  system was considerably lower than nano-emulsions of the other two systems; therefore, the higher stability near the HLB temperature could be due to the presence of a liquid-crystalline phase. It has been reported that emulsion stability is very low at temperatures close to the HLB temperature owing to the low interfacial tensions achieved, which enhance thermal fluctuations on the monolayers [7–11]; however, it should be noted that it is true when only liquid phases are involved in the phase equilibrium. When a liquid-crystalline phase is present, the stability is considerably enhanced at the HLB temperature. The evolution of the droplet size as a function of time allowed us to estimate the nano-emulsion stability. The radius,  $r$ , to the third power is plotted as a function of time for nano-emulsions obtained by the PIT method in water/( $C_{14}E_4 + C_{12}E_6$ )/decane and in water/( $C_{16}E_4 + C_{12}E_6$ )/decane systems at different  $W_1$  values in Figs. 6 and 7. The linear variation of  $r^3$  as a function of time indicates that the mechanism of instability can be attributed to Ostwald ripening. The Ostwald ripening rate obtained from the slope of the straight lines of Figs. 6 and 7 is shown in Fig. 8 as a function of  $W_1$ . The phase equilibrium is also indicated in Fig. 8. The more stable nano-emulsions are those where a liquid-crystalline phase is present. In the system containing  $(C_{12}E_4 + C_{12}E_6)$  mixtures, the Ostwald ripening rate was found to be about 2 orders of magnitude higher than that of the other two systems. Creaming followed by coalescence was also observed in that system.

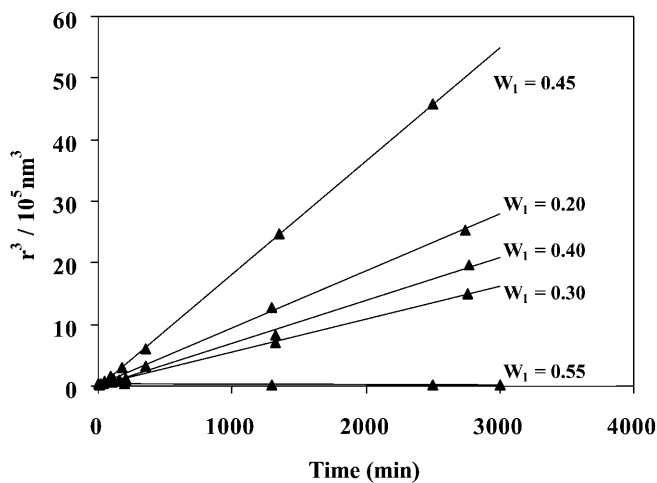


Fig. 6 Variation of  $r^3$  with time in emulsions of the water/ $(C_{14}E_4 + C_{12}E_6)$ /decane system prepared by the PIT method

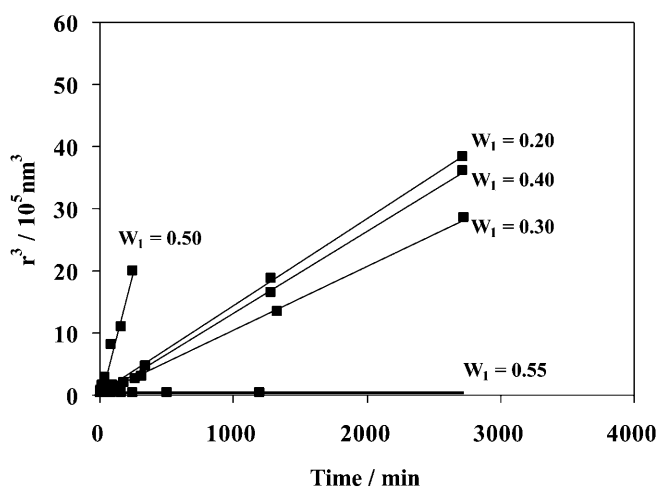


Fig. 7 Variation of  $r^3$  with time in emulsions of the water/ $(C_{16}E_4 + C_{12}E_6)$ /decane system prepared by the PIT method

## Conclusions

Nano-emulsions were obtained in a mixed surfactant system by two low-energy emulsification methods, PIT

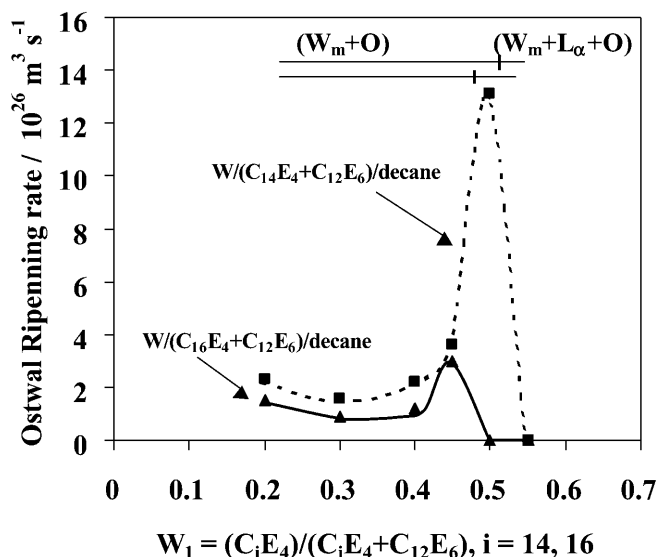


Fig. 8 Ostwald ripening rate as a function of  $W_1$  in emulsions of the water/ $(C_iE_4 + C_{12}E_6)$ /decane system,  $i = 12, 14, 16$ , obtained by the PIT method

and addition of water to a surfactant and oil solution (method B). The droplet size of the nano-emulsions obtained by the PIT method (in the range 60–80 nm) is independent of  $W_1$ . In contrast, the droplet size in emulsification method B (in the range 60–300 nm) is highly dependent on  $W_1$ .

Near  $T_{HLB}$ , where the equilibrium phases are  $(W_m + L_\alpha + O)$ , nano-emulsions obtained by the two methods have similar droplet size. The most stable nano-emulsions were obtained in the vicinity of  $T_{HLB}$  where the equilibrium phases are  $(W_m + L_\alpha + O)$ . The main mechanism of destabilization of nano-emulsions belonging to the  $(W_m + O)$  region is Ostwald ripening.

**Acknowledgements** The authors acknowledge financial support by CICYT (grant QUI 99-0997-CO2) and “Comissionat per a Universitats i Recerca, Generalitat de Catalunya” (grant 1999SGR-00193). A.F. acknowledges CONICIT-ULA for a Ph.D. grant.

## References

1. Becher P (1965) Emulsions: theory and practice. Reinhold, New York
2. Binks BP (1998) In: Binks BP (ed) Modern aspects of emulsion science. The Royal Society of Chemistry, Cambridge, pp 1–55
3. Shinoda K, Arai H (1964) J Phys Chem 68:3485
4. Shinoda K, Saito H (1968) J Colloid Interface Sci 26:70
5. Kunieda H, Shinoda, K (1985) J Colloid Interface Sci 17:107
6. Bourrel M, Schechter R (1988) In: Bourrel M, Schechter R (eds) Micro-emulsions and related systems, vol 30. Dekker, New York, pp 140–148
7. Shinoda K (1967) J Colloid Interface Sci 24:4
8. Saito H, Shinoda K (1970) J Colloid Interface Sci 32:647
9. Vinatieri JE (1980) Soc Pet Eng J 20:402
10. Kunieda H, Shinoda K (1982) Bull Chem Soc 55:1777
11. Kabalnov A, Weers J (1996) Langmuir 12:1931
12. Kunieda H (1992) In: Keizo O, Mas-hiko A (eds) Mixed surfactant systems. Surfactant science series, vol 46. Dekker, New York, pp 235–261

- 
13. Binks BP, Meunier J, Abillon O, Langevin D (1989) *Langmuir* 5:415
  14. Nakajima H (1997) In: Solans C, Kunieda H (eds) *Industrial applications of microemulsions*, vol 66, Dekker, New York, pp 175–197
  15. Lovell PA, El-Aasser MS (1997) In: Lovell PA, El-Aasser MS (eds) *Emulsion polymerization and emulsion polymers*. Wiley, Chichester, pp 697–722
  16. Benita S (1998) In: Benita S (ed) *Sub-micron emulsions in drug targeting and delivery*. Harwood, Amsterdam, p 338
  17. Taylor P, Ottewill RH (1994) *Prog Colloid Polym Sci* 97:199–203
  18. Katsumoto Y, Ushiki H, Mendibourne B, Graciaa A, Lachaise J (2000) *J Phys Condens Matter* 12:3569–3583
  19. Lifshitz IM, Slezov VV (1961) *J Phys Chem Solids* 19:35
  20. Wagner C (1961) *Ber Bunsenges Phys Chem* 66:581
  21. Kabalnov AS, Pertzov AV, Shchukin ED (1987) *Colloids Surf* 24:19
  22. Forgiarini A, Esquena J, Gonzalez C, Solans C (2000) *Prog Colloid Polym Sci* 115:36–39
  23. Kunieda H, Fukui Y, Uchiyama H, Solans C (1996) *Langmuir* 12:2136–2140
  24. Shinoda K (1967) *J Colloid Interface Sci* 14:4–9
  25. Kunieda H (1986) *J Colloid Interface Sci* 114:378–385